Influence of breakouts on borehole sonic dispersions

Ergun Simsek, Bikash K. Sinha, Smaine Zeroug, Schlumberger, and Noureddine Bounoua, Sonatrach

Summary

Borehole breakouts are commonly encountered during underbalance drilling in the presence of large tectonic stresses. The characteristics of borehole sonic data may be affected by strong departures from cylindrical geometry. A finite-difference time domain (FDTD) formulation with a perfectly-matched layer (PML) enables a study of the influence of breakouts on the borehole Stoneley, flexural and quadrupole dispersions. Breakout azimuths are oriented perpendicular to the maximum horizontal stress direction. The FDTD formulation yields synthetic waveforms at an array of receivers produced by a monopole, dipole or quadrupole source placed on the borehole axis. The borehole cross-section can be modified to simulate the breakout geometry. Synthetic waveforms are then processed by a modified matrix pencil algorithm to isolate both non-dispersive and dispersive arrivals in the wavetrain. While the axi-symmetric Stoneley dispersion is marginally affected by the presence of a breakout, there are discernible changes in both the flexural and quadrupole dispersions that can help in the analysis of such borehole failures. Computational results indicate that the presence of a symmetric breakout causes both the flexural and quadrupole wave splitting in the intermediate frequency band similar to the case of an elliptic hole. The two canonical dispersions approximately correspond to the largest and smallest diameters of the distorted borehole cross-section. These characteristic changes in the Stoneley, flexural and quadrupole dispersions can be used as indicators of the presence of breakouts and need to be accounted for in the sonic data inversion and interpretation.

Introduction

Borehole breakouts are compressive-shear failure of rocks in the presence of large tectonic stresses causing large compressive hoop stress at the borehole surface. Breakouts are more likely to occur during underbalance drilling or surge and swab operation performed by drillers. The breakout azimuth coincides with the minimum horizontal stress direction and the distorted borehole cross-section can be used to estimate the maximum horizontal stress magnitude (Bell and Gough, 1983; Zoback et al., 1985; Vernik and Zoback, 1992; Grandi and Toksöz, 2005). A detailed borehole cross-sectional image is obtained by a four-arm dipmeter and an ultrasonic imaging tool that operates in a pulse-echo mode (Plumb and Hickman, 1985).

Borehole cross-section affects the propagation of guided modes, such as the lowest-order axi-symmetric Stoneley, flexural, and quadrupole modes. Changes in the borehole cross-section can be identified by monitoring perturbations in the guided mode dispersions from a reference circular borehole case. This paper presents a study of the influence of borehole breakouts on the Stoneley, flexural, and quadrupole modes using the FDTD method with a PML to minimize reflections from the outer boundary. Synthetic waveforms at an array of receivers are processed by a modified matrix pencil algorithm to identify both non-dispersive and dispersive arrivals in the wavetrain (Ekstrom, 1995). We relate breakout parameters to changes in borehole dispersions, as well as demonstrate flexural and quadrupole wave splittings into two canonical dispersions.

Theory

Breakouts can cause complex perturbations to the borehole cross-section that have a significant influence on borehole dispersions. A typical breakout cross-section exhibits a symmetric elongation of borehole along the minimum horizontal stress direction and negligibly small perturbation along the maximum horizontal direction. While non-symmetric distortion of boreholes are also known to occur, we plan to analyze in this paper symmetric breakouts that lead to splitting of flexural waves into two canonical waves corresponding to the long and short diameters of the distorted borehole.

We analyze wave propagation in wellbores with symmetric breakouts using a finite-difference formulation of equations of motion in 3D-cylindrical coordinates (Liu and Sinha, 2003). This formulation enables us to introduce any cross-sectional geometry of the borehole together with an equivalent structure to account for the sonic tool effects on the Stoneley, flexural, and quadrupole dispersions (Pistre et al., 2005).

Computational results in a fast formation

Based on measured slownesses in a fast formation in North Africa, we use the following material parameters in the FDTD calculations of synthetic waveforms. The formation compressional and shear velocities are 5102.1 and 3384.4 m/s, respectively, whereas the mass density is 2200 kg/m^3. The borehole fluid compressional velocity is 1454 m/s, and its mass density is 1000 kg/m^3. The circular borehole diameter is 22.08 cm. We consider borehole elongations of varying amounts along the breakout azimuth and compute synthetic waveforms generated by a monopole, dipole and quadrupole transmitters.

Figure 1 shows a schematic diagram of borehole in the presence of stress-induced breakouts. Figure 2

displays a cross-sectional view of an elongated borehole together with an equivalent concentric heavy-fluid column used in the FDTD calculations of synthetic waveforms. The outer cylindrical layer represents an isotropic and homogeneous formation as included in the finite-difference calculations with a PML at the outer boundary. We have recorded synthetic waveforms at 20 receivers with an inter-receiver spacing of 10 cm and used a mode-order of 4 in a modified matrix pencil algorithm to obtain borehole dispersions. In Figure 3, we show the Stoneley (in blue) , flexural (in green) and quadrupole (in red) dispersions obtained from synthetic waveforms generated by a monopole, dipole, and quadrupole sources placed outside the heavy-fluid column. The dipole and quadrupole transmitters are aligned parallel to the breakout azimuth that is perpendicular to the maximum stress direction. The dashed and solid black curves, respectively, denote the Stoneley, flexural and quadrupole dispersions obtained from a mode-search routine for circular boreholes of radii 11.04 and 12.88 cm. Notice that borehole dispersions obtained using a breakout cross-sectional shape of borehole are remarkably close to those from a circular borehole with its diameter equal to the elongated diameter in the presence of a breakout. Figure 4 depicts similar results for the borehole dispersions obtained synthetic waveforms generated by placing the dipole and quadrupole transmitters perpendicular to the elongated diameter. Under these circumstances, the Stoneley, dipole and quadrupole dispersions closely correspond to borehole dispersions for a circular borehole with its diameter equal to the short diameter of the distorted borehole cross-section in the presence of a breakout. However, the axi-symmetric Stoneley, quadrupole and pseudo-Rayleigh dispersions remain essentially the same as in the case of transmitters aligned parallel to the elongated diameter. Results from Figures 3 and 4 suggest that the axi-symmetric Stoneley, pseudo-Rayleigh (n=0), and quadrupole (n=2) modes do not show any difference between the two transmitter orientations relative to the elongated borehole diameter.

When we place the dipole and quadrupole transmitters at 45 degrees from the elongated diameter, we obtain borehole dispersions corresponding to two circular boreholes with both the largest and smallest diameters of the distorted borehole. Figure 5 shows modal dispersions obtained from synthetic waveforms generated a single firing of monopole, dipole, and quadrupole transmitters oriented at 45 degrees to the breakout azimuth. This observation confirms that the presence of a symmetric breakout causes flexural wave splitting into two canonical dispersions that correspond to the long and short diameters of the distorted borehole cross-section. These results also suggest that while the flexural waves are sensitive to the azimuth of the elongated borehole diameter, quadrupole waves are essentially insensitive to the orientation of a symmetric breakout.

All of these results indicate that the presence of a symmetric breakout causes a significant perturbation of flexural and quadrupole dispersions in the intermediate frequency band near the Airy's phase where the excitation amplitude is large. However, there are no changes in the dipole and quadrupole dispersions at very low and high frequencies where borehole cross-section is known to have negligible effect on modal dispersions.

Next we analyze the influence of breakout parameters on the amount of perturbations in borehole dispersions in the intermediate frequency band. Borehole breakouts can be characterized in terms of the angular spread and borehole diameter elongation.

Computational results indicate that the presence of a typical breakout in a fast formation has a negligibly small (less than 2%) effect on the Stoneley dispersion. In contrast, we notice a significant amount of dipole-shear wave splitting in the intermediate frequency band. The solid curves in Figure 6 show fractional changes in the flexural slowness as a function of frequency for different borehole elongations relative to the short diameter of the distorted cross-section. The angular spread of breakout is fixed at 30 degrees. Notice that the peak perturbation in the flexural wave slowness occurs around 3.2 kHz and it increases with increasing amount of elongation. A 25% elongation of borehole diameter along the breakout azimuth causes a maximum of about 45% change in the flexural wave slowness in a typical fast formation in North Africa. The dashed curves denote fractional changes in the flexural wave slowness computed from a mode-search routine for circular boreholes with diameters equal to the largest and smallest diameters of distorted cross-section in the presence of a breakout. Figure 7 displays similar results for the quadrupole dispersion as those shown in Figure 6 for the dipole-flexural dispersion. A major difference in the response of a quadrupole mode from that for a dipole-flexural mode is that larger changes in the quadrupole dispersion occur at higher frequencies. Notice that the largest change in the quadrupole dispersion occurs around 6 kHz for the chosen formation parameters.

Next we describe the influence of increasing angular spread of breakout for a given amount of borehole elongation in a fast formation. Figure 8 depicts fractional changes in the flexural wave slowness as a function of frequency for angular spreads of 36, 60, 90, and 108 degrees. As is the case in Figure 6, large changes in the flexural wave slowness occur in the vicinity of 3.2 kHz. In Figure 9, we show similar results for fractional changes in the quadrupole slowness as a function of frequency for different amounts of angular spread.

Summary and Conclusions

We have used a 3D cylindrical FDTD with PML formulation of the linear equations of motion to simulate

effects of breakout-induced deformation of the borehole cross-section on borehole dispersions.

We have demonstrated that a symmetric borehole breakout in a fast formation produces characteristic signatures associated with the Stoneley, dipole, and quadrupole dispersions. While the borehole Stoneley is marginally affected, dipole flexural and quadrupole dispersions are significantly perturbed in the intermediate frequency band. When the dipole transmitter is oriented parallel and perpendicular to the breakout azimuth, the corresponding flexural dispersions approximately coincide with dispersions for the largest and smallest diameters of the deformed borehole cross-section, respectively.

Both the dipole flexural and quadrupole dispersions are significantly affected by a typical borehole elongation caused by the presence of a symmetric breakout. In contrast, angular spread of the breakout geometry causes a rather small amount of perturbations in the flexural and quadrupole dispersions in the intermediate frequency band. Computational results indicate that a given breakout causes relatively smaller perturbations in the Stoneley, flexural and quadrupole dispersions in a slow formation than that in a fast formation.

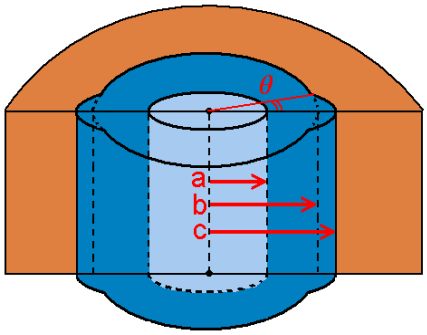

Figure 1. Schematic diagram of a borehole in the presence of a breakout with an angular spread of 2θ. The heavy-fluid column radius is denoted by "a". The short and long radii of the distorted borehole are given by "b" and "c", respectively.

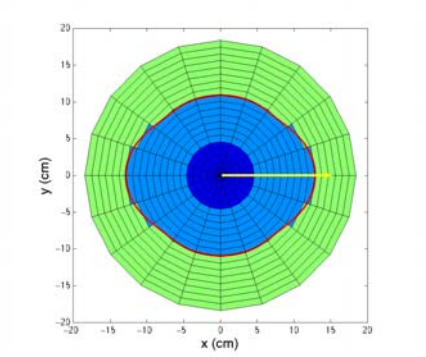

Figure 2. Cross-sectional view of a borehole in the presence of a breakout parallel to the x-axis. A heavy-fluid column on the borehole axis is used to simulate the sonic tool effects on borehole dispersions. The thin red line depicts the approximated borehole in the presence of a breakout, and the yellow arrow shows the firing direction.

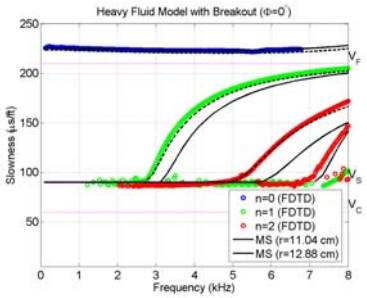

Figure 3. Monopole (blue dots), dipole (green dots), and quadrupole (red dots) dispersions obtained by FDTD method for a heavy-fluid model with an inline breakout. Mode Search (MS) results are for the short and long two radii of the distorted borehole. The dashed and solid lines correspond to boreholes of radii 12.88 and 11.04 cm, respectively.

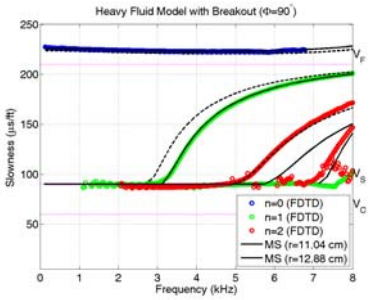

Figure 4. Monopole (blue dots), dipole (green dots), and quadrupole (red dots) dispersions obtained by FDTD method for a heavy-fluid model with a crossline breakout. Mode-search (MS) results are for the short and long radii of the distorted borehole. The dashed and solid lines correspond to boreholes of radii 12.88 and 11.04 cm, respectively.

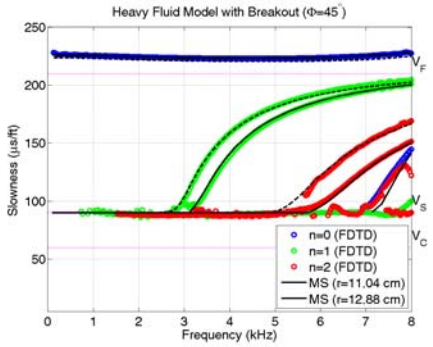

Figure 5. Monopole (blue dots), dipole (green dots), and quadrupole (red dots) dispersions are obtained by FDTD method for a heavy-fluid model with a deviated breakout. Mode-search (MS) results are for two different radii.

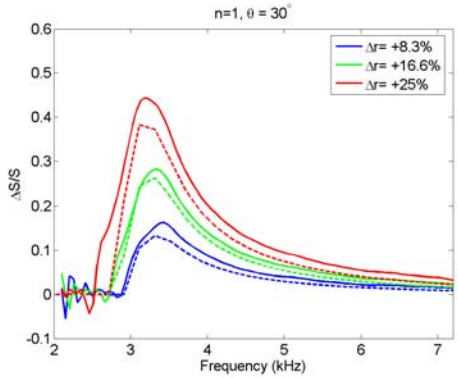

Figure 6. Fractional changes in the flexural wave slowness for different amounts of borehole diameter elongations. The red, green, and blue curves represent results for 8.3, 16.6, and 25% elongations of the long diameter of the distorted borehole. The dashed curves denote results from a mode-search routine for circular boreholes with the short and long diameters of the distorted borehole.

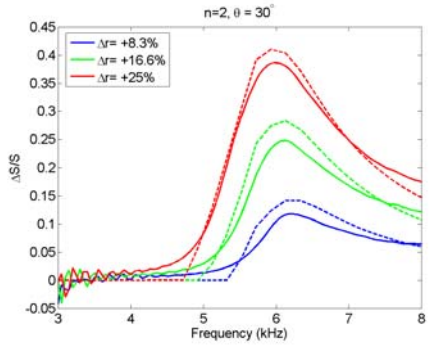

Figure 7. Fractional changes in the quadrupole wave slowness for different amounts of borehole diameter elongations. The notation is the same as in Figure 6.

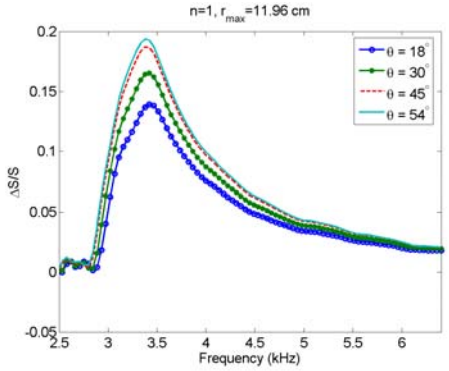

Figure 8. Fractional changes in the flexural wave slowness for a fixed borehole elongation of 8.3% and different amounts of angular spread.

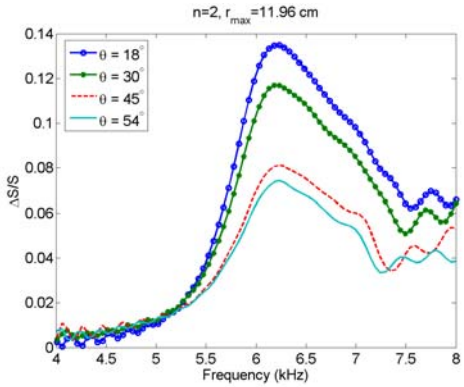

Figure 9. Fractional changes in the quadrupole wave slowness for a fixed borehole elongation of 8.3% and different amounts of angular spread.

EDITED REFERENCES

Note: This reference list is a copy-edited version of the reference list submitted by the author. Reference lists for the 2007 SEG Technical Program Expanded Abstracts have been copy edited so that references provided with the online metadata for each paper will achieve a high degree of linking to cited sources that appear on the Web.

REFERENCES

Bell, J. S., and D. I. Gough, 1983, The use of borehole breakout in the study of crustal stress, in M. D. Zoback and B. C. Haimson, eds., Hydraulic fracturing stress measurements: National Academic Press, 201–209.

Ekstrom, M. E., 1995, Dispersion estimation from borehole acoustic arrays using a modified matrix pencil algorithm: Presented at the 29th Asilomar Conference on Signals, Systems and Computations, IEEE.

Grandi, S., and N. Toksoz, 2005, In-situ stress field from borehole measurements and plate tectonic models: Presentd at the Spring Meeting, AGU.

Liu, Q. H., and B. K. Sinha, 2003, A 3D cylindrical PML/FDTD method for elastic waves in fluid-filled pressurized boreholes in triaxially stressed formations: Geophysics, 68, 1731–1743.

Pistre, V., Kinoshita, T., Endo, T., Schilling, K., Pabon, J., Sinha, B., Plona, T., Ikegami, T., and Johnson, D., 2005: A modular wireline sonic tool for measurements of 3D (azimuthal, radial, and axial) formation acoustic properties, 46th Annual Society of Professional Well Log Analysts Symposium, New Orleans, LA, June 27-29.

Plumb, R. A., and S. H. Hickman, 1985, Stress-induced borehole enlargement: a comparison between the four-arm dipmeter and the borehole televiewer in the Auburn geothermal well: Journal of Geophysical Research, 90, 5513–5522.

Vernik, L., and M. D. Zoback, 1992, Estimation of maximum horizontal principal stress magnitude from stress-induced wellbore breakouts in the Cajon Pass Scientific Research Borehole: Journal of Geophysical Research, 97, 5109–5119.

Zoback, M. D., D. Moos, L. Mastin, and R. N. Anderson, 1985, Wellbore breakouts and in-situ stress: Journal of Geophysical Research, 90, 5523–5530.